Bioorganic Chemistry 90 (2019) 103086

Contents lists available at ScienceDirect

Bioorganic Chemistry

journal homepage: www.elsevier.com/locate/bioorg

Design, synthesis and biological evaluation of novel thieno[3,2-*d*] pyrimidine and quinazoline derivatives as potent antitumor agents

Hao Hu, Yuhong Dong, Ming Li, Ruxin Wang, Xian Zhang, Ping Gong*, Yanfang Zhao*

Key Laboratory of Structure-Based Drug Design and Discovery (Shenyang Pharmaceutical University), Ministry of Education, 103 Wenhua Road, Shenhe District, Shenyang 110016, PR China

Department of Pharmacology, Shenyang Pharmaceutical University, 103 Wenhua Road, Shenhe District, Shenyang 110016, PR China

ARTICLE INFO

Keywords:
Thieno[3,2-*d*]pyrimidine
Quinazoline
Synthesis
Antitumor activity

ABSTRACT

Four series of novel thieno[3,2-*d*]pyrimidine and quinazoline derivatives containing *N*-acylhydrazone or semicarbazone were designed, synthesized, and evaluated for their biological activity. Of which compound **14** showed the most potent antitumor activities with IC_{50} values of 1.78 μM, 1.02 μM, 1.98 μM, 0.41 μM and 0.22 μM against HT-29, MDA-MB-231, U87MG, PC-3 and HCT-116 cell lines respectively. Inhibition of enzymatic assays showed that PI3Kα was very likely to be one of the drug targets of **14** with the IC_{50} value of 0.20 μM. According to the results of antitumor activity, the SARs were summarized, which indicated that thieno[3,2-*d*]pyrimidine and semicarbazone are optimal fragments. In addition, compounds with hydroxyl group at the 4-position on the terminal phenyl ring were more active. Annexin-V and propidium iodide (PI) double staining confirmed that the most active cytotoxic compound **14** can induce cell apoptosis in HCT-116 cells. Moreover, the influence of **14** on the cell cycle distribution was assessed on the HCT-116 cell line, exhibiting a cell cycle arrest at the G2/M phase. Furthermore, molecular docking analysis was also performed to determine possible binding modes between PI3Kα and the target compound. These results will guide us to further refine the structure of the thieno[3,2-*d*]pyrimidine and quinazoline derivatives to achieve optimal antitumor activity.

1. Introduction

The understanding of the molecular mechanism for cancer has been dramatically progressed over the last decade. Protein-targeted cancer therapies have also become easier and more popular due to advances in molecular biology. As a family of lipid kinases, phosphoinositide 3-kinases (PI3Ks) play a central role in cellular activities such as growth, transformation, proliferation, motility and differentiation [1,2]. PI3Ks phosphorylate phosphatidylinositol 4,5-bisphosphate (PIP2) at the 3-OH of the inositol ring to generate phosphatidylinositol 3,4,5-trisphosphate (PIP3), which in turn activates Akt and the downstream effectors like mTOR, therefore give the anticancer effect [3–5].

Recently, accumulating evidences have illustrated that substituted thieno[3,2-*d*]pyrimidines and quinazolines present in the cores of many physiologically active agents, due to their broad bioactivities including antitumor [6–10], antimicrobial [11], and anti-inflammatory activity [12]. Of these active compounds (Fig. 1), GDC-0941, which is a potent, selectively, orally bioavailable inhibitor of PI3K is currently undergoing phase I clinical trials for the treatment of PIK3CA-mutant breast cancer [13,14]. Moreover, Idelalisib, which has the quinazoline core had been launched in July 2014 in the U.S for the treatment of relapsed chronic lymphocytic leukemia as a phosphatidylinositol 3-kinase delta (PI3K-delta) inhibitor [10,15]. Their structure-activity relationships (SARs) studies revealed that the morpholino substituted thieno[3,2-*d*]pyrimidine or quinazoline scaffolds play a key role in their antitumor activities [7–10,16,17].

Over the last two decades the bioactive *N*-acylhydrazone (NAH) core has been prevailing among the most ubiquitous functional group in medicinal chemistry and identified in a huge number of hits which act on various types of molecular targets [18–23]. PAC-1 which is a NAH small scaffold procaspase activator discovered in 2006 demonstrated promising anticancer action both in *in vitro* and *in vivo* models [24]. Thus, the development of such small molecules with NAH framework, which can readily bind with various enzymes and receptors in organisms through forming hydrogen bond interactions, has been shown to be a feasible antitumor strategy.

In view of these observations, on the basis of association principle, we combined the thieno[3,2-*d*]pyrimidine and quinazoline

* Corresponding authors at: Key Laboratory of Structure-based Drug Design and Discovery, Ministry of Education, Shenyang Pharmaceutical University, Shenyang 110016, PR China.

E-mail addresses: gongpinggp@126.com (P. Gong), yanfangzhao@126.com (Y. Zhao).

https://doi.org/10.1016/j.bioorg.2019.103086
Received 27 March 2019; Received in revised form 21 June 2019; Accepted 25 June 2019
Available online 26 June 2019

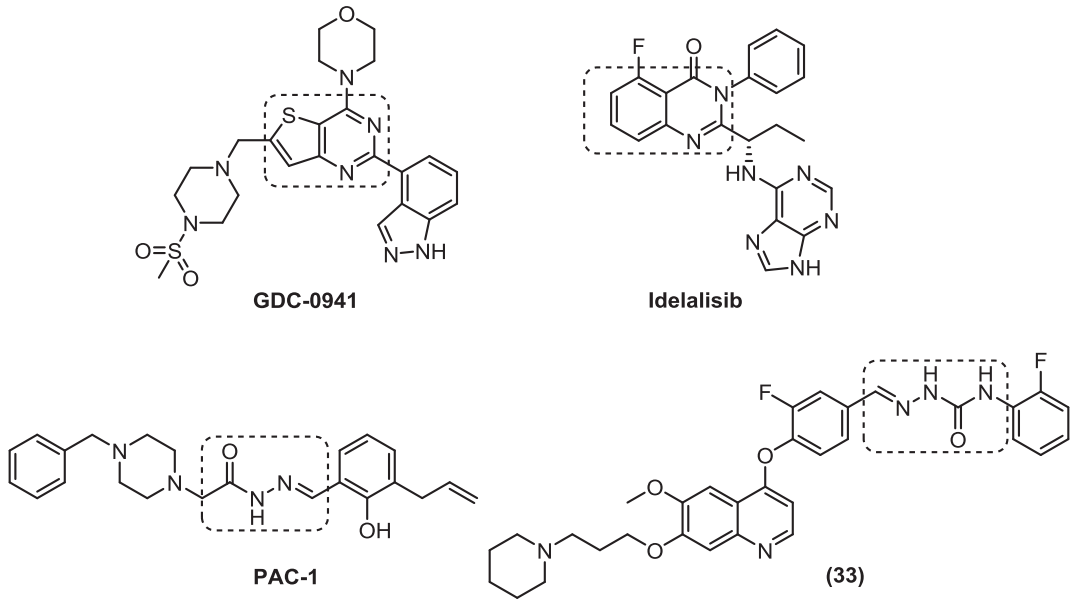

Fig. 1. Structures of representative kinase inhibitors.

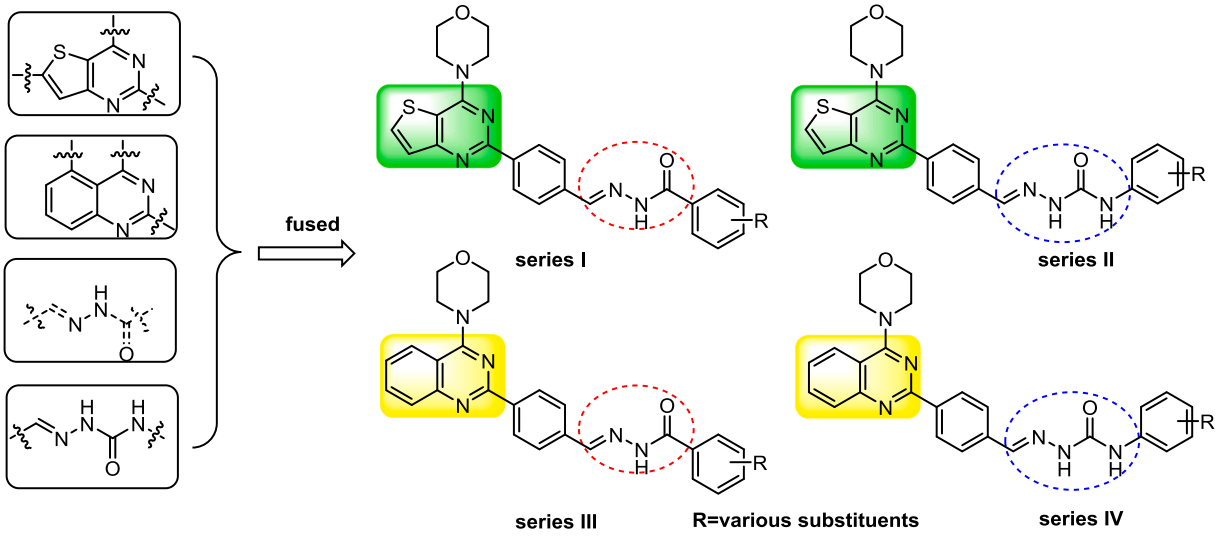

Fig. 2. Design strategy for the target compounds.

pharmacophores with the NAH framework. Therefore, two series of compounds were designed and synthesized. Moreover, in our previous study of 4-phenoxyquinoline derivatives, we found that compound **33** [25], which bearing semicarbazone linker, exhibited potent anti-proliferative activity as a c-Met inhibitor. Thus, on the molecular design level, by introducing semicarbazone scaffold the design is expected to exert more hydrogen-bond interactions with receptors. Further modifications were also performed by introducing various substituents to the terminal phenyl ring with the purpose of exploring the influence of substituents on anticancer activity by regulating the electronic and steric effects (Fig. 2).

2. Results and discussion

2.1. Chemistry

2.1.1. Synthesis of target compounds *4–26*

All target compounds listed in Fig. 2 were prepared as shown in Schemes 1–3 from the key intermediate $\mathbf{A_1}$ and $\mathbf{A_2}$ respectively. Commercially available methyl 3-aminothiophene-2-carboxylate reacted with urea in molten to provide the intermediate **a**, which was then chlorinated using phosphorus oxychloride to afford intermediate **b**. Intermediate **c** was obtained via substitution reaction in the presence of morpholine, then performing a Suzuki coupling with (4-formylphenyl) boronic acid to yield the key intermediate $\mathbf{A_1}$ [26,27]. The synthesis method of $\mathbf{A_2}$ is the same as that of $\mathbf{A_1}$ outlined in Scheme 1.

The intermediate $\mathbf{B_1}$-$\mathbf{B_3}$ and $\mathbf{C_1}$-$\mathbf{C_{13}}$ were synthesized as outlined in Scheme 2. The substituted methyl benzoate reacted with hydrazine hydrate to obtain the intermediate $\mathbf{B_1}$-$\mathbf{B_3}$. The substituted aniline reacted with phenyl chloroformate and then treated with hydrazine hydrate to obtain the intermediate $\mathbf{C_1}$-$\mathbf{C_{13}}$. As described in Scheme 3, intermediates $\mathbf{A_1}$ and $\mathbf{A_2}$ were treated with intermediates $\mathbf{B_1}$-$\mathbf{B_3}$ or $\mathbf{C_1}$-$\mathbf{C_{13}}$ to afford the target compounds respectively.

2.1.2. Structural confirmation of target compounds

All the target compounds were purified by column chromatography on silica gel. The chemical structures of the target compounds were confirmed by mass spectrometry and NMR. In order to determine the relative configuration of the target compounds, the NOESY experiment of compound **12** was carried out and an evident NOE signal was

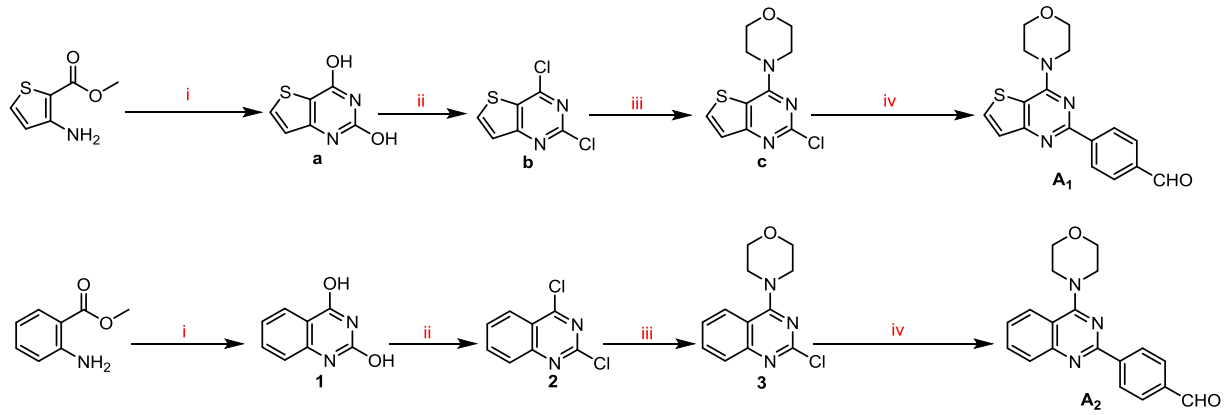

Scheme 1. Reagents and conditions: (i) urea, 200 °C, 2 h; (ii) $POCl_3$, 80 °C, 8 h; (iii) morpholine, CH_3OH, rt, 2 h; (iv) (4-formylphenyl)boronic acid, $Pd(PPh3)_2Cl_2$, Cs_2CO_3, Dioxane, H_2O, 80 °C, 5 h.

observed between the proton H_1 (7.98 ppm) and the proton H_2 (10.86 ppm). Therefore, we proved that the double bond of compounds **4–26** is the *E* configuration (see Figs. 3 and 4).

2.2. Biological evaluation

2.2.1. In vitro cytotoxic activities and structure-activity relationships

The cytotoxic activities of the synthesized compounds **4–26** were evaluated in HT-29 (human colon cancer), MDA-MB-231 (human breast cancer), U87MG (human glioblastoma), PC-3 (human prostate cancer) and HCT-116 (human colon cancer) cell lines by applying the 3-[4,5-dimethylthiazol-2-yl]-2,5-diphenyl-2H-tetrazolium bromide (MTT) colorimetric assay. GDC-0941 was used as the positive control. The results of the mean values of experiments performed in triplicate, expressed as half maximal inhibitory concentration (IC_{50}) values, were summarized in Table 1.

The SARs on series **I** and series **III** were firstly studied. Compound **6** with methoxyl group on the phenyl ring exhibited better activity than compound **4** with electron-withdrawing group on the phenyl ring. The same regularity can be seen from compounds **16** and **17**, whereas compound **5** bearing the hydroxyl group resulted in a 2.2–22.6 fold increase in the potency against five cell lines compared to compound **6**. This could demonstrate that small sized substituents at the 4-position of the phenyl ring is also needed.

Further studies were performed to determine which position affects activity. When comparing series **II** with **IV**, the results showed that when electron-donating groups or electron-withdrawing groups were introduced to 2 position of the phenyl ring, the compounds had a dramatic loss in activity, which could be confirmed by compounds (**13** and **15** *vs* **12**) and (**22** and **24** *vs* **23**), suggesting that it is better to have no substitution at this region. For series **II**, compound **11** with a fluorine on the 3-position of the phenyl ring led to an obvious improvement in antitumor activity than compound **12** against MDA-MB-231, U87MG, PC-3 and HCT-116 cell lines. The introduction of methoxy group surely improved the activity (**26** *vs* **23**), whereas it has the opposite result for series **IV**. Further analysis revealed clearly that the size of the substituents had mainly influence on the activity of the 4-position. It was noted that the larger size substituents decreased the potency. For example, the cytotoxicity of compound **8** decreased much against the five cancer cell lines because of the larger size of isopropyl at the 4-position. However, compound **14** has the same electron-donating property exhibited superior activity even compared with the positive control GDC-0941. For series **IV**, another interesting phenomenon is that the introduction of strong electron-donating groups into the 2,4-position led to an unexpected improvement of activity against MDA-MB-231, PC-3 and HCT-116 cell lines (**19** *vs* **23**).

Interestingly, most of the compounds were more potent against MDA-MB-231, U87MG and HCT-116 cell lines than the other two cancer cell lines (HT-29 and PC-3). It is not difficult to draw the conclusion that most of the compounds bearing thieno[3,2-*d*]pyrimidine ring with the semicarbazone scaffold as the linker behave better activities than the other three series compounds. According to the pharmacological data, we concluded that a substitutent with proper degree of electron density and suitable size on the terminal phenyl ring is beneficial to achieve better antitumor activity.

Overall, the activities of most of these compounds were similar or even higher than that of GDC-0941 against one or more cancer cell lines. Among them compounds **14** exhibited the best activity against all of the tested cell lines with IC_{50} values of 1.78 μM, 1.02 μM, 1.98 μM, 0.41 μM and 0.22 μM against HT-29, MDA-MB-231, U87MG, PC-3 and HCT-116 cell lines respectively, indicating it has a promising potential for further exploration.

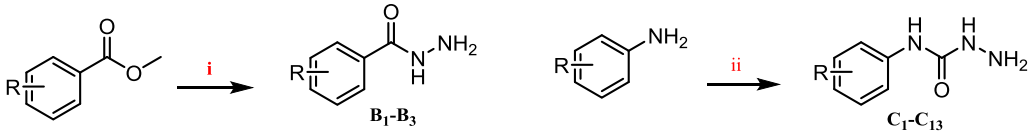

B_1:R=4-F; B_2:R=4-OH; B_3:R=4-OCH_3

C_1:R=3,4-$(Cl)_2$; C_2:R=4-$CH(CH_3)_2$; C_3:R=4-F;

C_4:R=2,4-$(OCH_3)_2$; C_5:R=3-F; C_6:R=H; C_7:R=2-CH_3; C_8:R=4-OH;

C_9:R=2-Cl ; C_{10}:R=4-Br; C_{11}:R=2-CF_3; C_{12}:R=3-CF_3; C_{13}:R=3-OCH_3

Scheme 2. Reagents and conditions: (i): $NH_2NH_2{\cdot}H_2O$ (80%), toluene, 80 °C, 2 h; (ii) a: phenyl carbonochloridate, pyridine, DCM, 0 °C, 5 h; b: $NH_2NH_2{\cdot}H_2O$ (80%), toluene, 80 °C, 2 h.

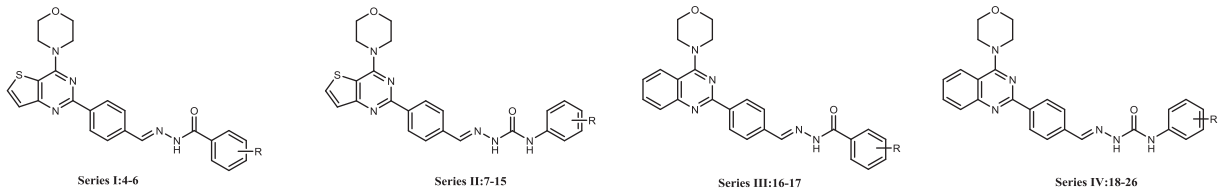

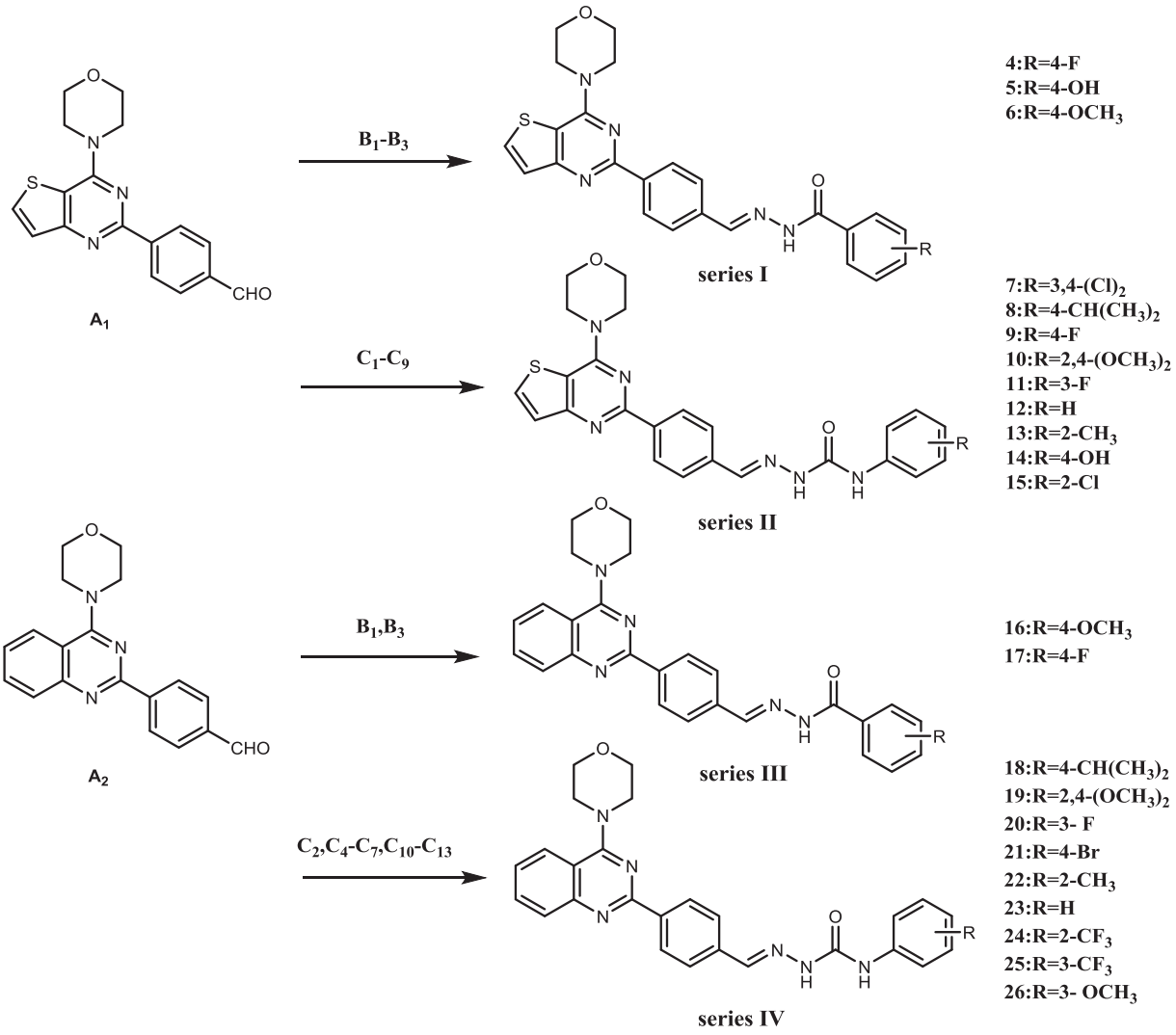

Scheme 3. Reagents and conditions: EtOH, rf, 2 h.

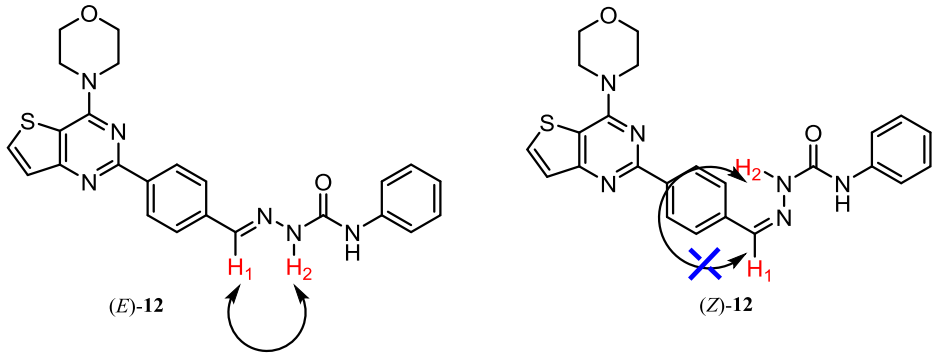

Fig. 3. NOESY effect of the representative compound **12**.

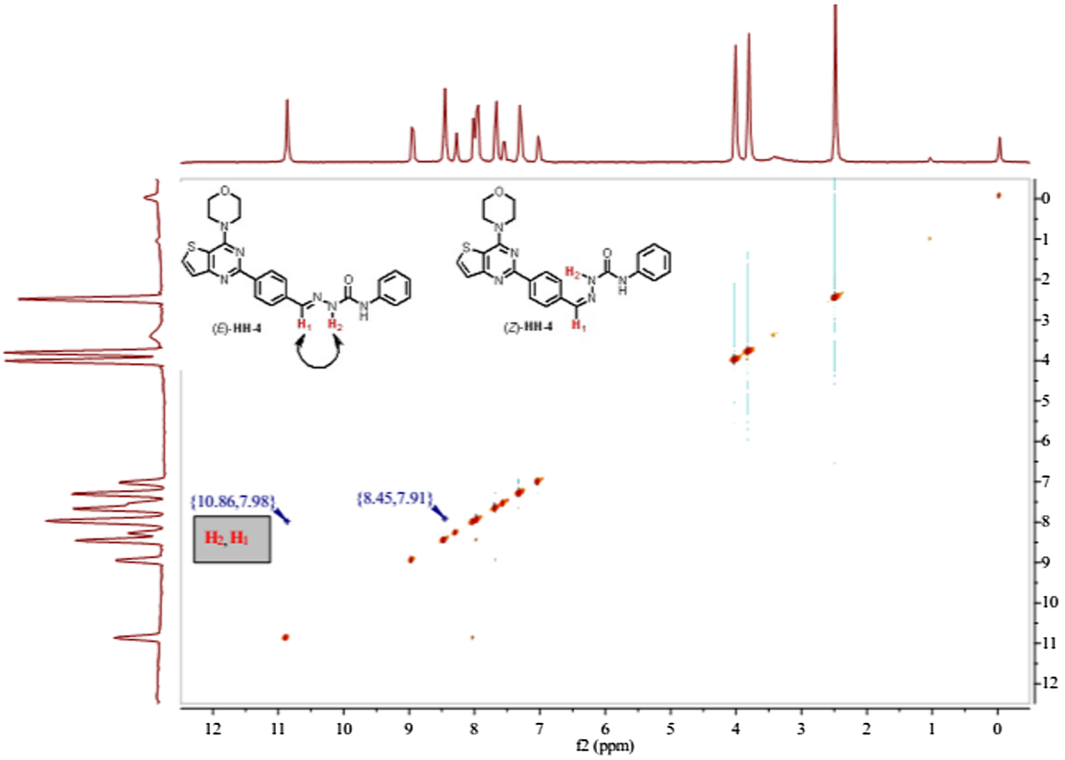

Fig. 4. 2D NOESY spectrum of representative compound **12**.

2.2.2. PI3Kα and mTOR enzymatic activity assay

To investigate their molecular mechanisms of action preliminarily, the selected compound **14** was further evaluated for eight selected kinases, which are probable biological targets for the designed compounds [6–12]. GDC-0941 was used as the positive drug. The results are listed in Table 2. As shown below, compound **14** inhibited PI3Kα kinase with IC_{50} values of 0.20 μM, whereas the impact on the other kinases was negligible. Even though it showed some selectivity against PI3Kα, the inhibitory activity of the compound **14** was still much weaker than GDC-0941.

2.2.3. Cell apoptosis study

To investigate the molecular mechanisms of action preliminarily, we performed an apoptosis experiment of compound **14** in the HCT-116

Table 1
Cytotoxicity of 4–26 against HT-29, MDA-MB-231, U87MG, PC-3, and HCT-116 cell lines in vitro.

Compd.	R	IC_{50}[a] (μmol/L) ± SD				
		HT-29	MDA-MB-231	U87MG	PC-3	HCT-116
4	4-F	> 100	31.47 ± 2.40	9.02 ± 0.39	> 100	18.45 ± 1.02
5	4-OH	4.37 ± 0.13	4.09 ± 0.20	1.56 ± 0.12	1.65 ± 0.15	1.72 ± 0.24
6	4-OCH_3	99.26 ± 4.02	16.02 ± 2.13	47.84 ± 3.10	23.32 ± 1.15	4.50 ± 0.32
7	3,4-$(Cl)_2$	> 100	34.47 ± 3.11	6.41 ± 0.35	> 100	24.87 ± 1.59
8	4-$CH(CH_3)_2$	> 100	18.46 ± 2.29	17.64 ± 1.12	10.22 ± 1.31	15.05 ± 1.89
9	4-F	25.52 ± 2.03	1.10 ± 0.14	4.37 ± 0.33	23.23 ± 3.33	0.18 ± 0.02
10	2,4-$(OCH_3)_2$	15.68 ± 2.01	1.31 ± 0.11	1.84 ± 0.22	1.50 ± 0.18	8.25 ± 0.42
11	3-F	17.62 ± 2.01	3.01 ± 0.21	1.28 ± 0.04	1.88 ± 0.42	1.72 ± 0.12
12	H	9.11 ± 0.11	10.23 ± 0.81	4.50 ± 0.19	3.12 ± 0.41	2.36 ± 0.29
13	2-CH_3	15.04 ± 0.13	18.15 ± 2.10	14.38 ± 3.21	45.08 ± 3.14	15.05 ± 1.21
14	**4-OH**	**1.78 ± 0.05**	**1.02 ± 0.03**	**1.98 ± 0.10**	**0.41 ± 0.11**	**0.22 ± 0.03**
15	2-Cl	> 100	18.44 ± 1.11	10.47 ± 2.03	13.11 ± 1.50	**12.47** ± 1.36
16	4-OCH_3	5.34 ± 0.24	12.51 ± 1.56	4.22 ± 0.43	18.48 ± 2.33	18.50 ± 3.43
17	4-F	> 100	22.34 ± 2.01	13.04 ± 1.04	6.23 ± 0.54	17.80 ± 1.21
18	4-$CH(CH_3)_2$	42.21 ± 5.04	1.78 ± 0.15	8.69 ± 1.11	0.86 ± 0.13	3.45 ± 0.19
19	2,4-$(OCH_3)_2$	25.65 ± 0.95	1.81 ± 0.11	8.37 ± 0.58	0.44 ± 0.03	0.50 ± 0.08
20	3- F	29.30 ± 2.02	22.62 ± 2.40	17.35 ± 1.24	32.47 ± 2.41	17.75 ± 2.05
21	4-Br	13.22 ± 0.96	5.38 ± 0.20	7.41 ± 0.63	2.84 ± 0.21	4.12 ± 0.33
22	2-CH_3	> 100	18.70 ± 1.54	47.23 ± 5.32	0.32	5.34 ± 0.27
23	H	11.69 ± 0.42	12.01 ± 0.81	3.63 ± 0.72	4.94 ± 0.68	12.50 ± 0.70
24	2-CF_3	> 100	23.01 ± 2.29	17.20 ± 1.74	40.56 ± 6.02	33.72 ± 3.04
25	3-CF_3	> 100	3.52 ± 0.11	10.56 ± 1.19	2.50 ± 0.46	4.22 ± 0.19
26	3-OCH_3	9.27 ± 0.53	3.05 ± 0.19	6.82 ± 1.01	1.87 ± 0.19	1.98 ± 0.21
GDC-0941[b]	–	0.59 ± 0.09	11.04 ± 0.58	16.01 ± 1.12	0.70 ± 0.16	0.30 ± 0.06

[a] Data presented is the mean ± SD value of three independent determinations.
[b] Used as a positive control.

Table 2
Inhibition of enzymatic assays by compound 14 *in vitro*.

Compd.	IC_{50}[a] in μM							
	PI3Kα	mTOR	B-Raf	C-Raf	EGFR	VEGFR	FLT3	KIT
14	0.20	9.80	> 10	> 10	> 10	> 10	4.80	> 10
GDC-0941[b]	0.003	–	–	–	–	–	–	–

[a] Data presented is the mean ± SD value of two independent determinations.
[b] Used as a positive control.

cell line using Annexin-V and propidium iodide (PI) double staining by flow cytometry and treating the HCT-116 cells with 0.5 μM, 1 μM and 5 μM of **14** for 48 h. The results can be seen in Fig. 5, which showed **14** is very effective in the induction of apoptosis in a dose-dependent manner. Compound **14** proved to induce apoptosis by 10.1% as compared to 1.7% of apoptotic cells in the untreated control (Table 3).

2.2.4. Cell cycle analysis

To better elucidate antitumor the mechanism responsible for antiproliferation and induction of apoptosis of compound **14**, we examined its effect on cell cycle. After treatment of HCT-116 cells with **14** for 48 h at indicated concentrations (0.5 μM, 1.0 μM, 5.0 μM), the cells were fixed and stained with PI, the DNA content was analyzed by flow cytometry. The obtained results were compared with non-treated HCT-116 cells as control. As shown in Fig. 6 treatment of HCT-116 cells with compound **14** at 0.5 μM, 1.0 μM, and 5.0 μM concentrations increased the percentage of G2/M − phase cells from 8.12% (control group) to 11.71%, 17.40%, and 20.56%, which indicate compound **14** impact in a dose dependent manner. These results confirmed that compound **14** significantly caused G2/M-phase arrest in HCT-116 cells (see Fig. 7).

2.2.5. Binding model analysis

To further elucidate the binding mode, a modeling study of **14** docked in PI3Kα homology model (PDB ID:4L23) based on PI3Kα crystal structures was performed. As showed in Fig. 8 **(A)**, the oxygen atom of morpholine formed one H-bond interactions with residue VAL851. In addition, the oxygen and nitrogen atoms of semicarbazone formed three H-bond interactions with residue LYS802 and residue ASP806, respectively. Its favorable biologic activity might be attributed to the presence of hydrogen bond donors and acceptors of semicarbazones. What is more, hydroxyl at the 4-position of the terminal phenyl ring formed one H-bond interaction with residue GLU1012, it's clear that this hydrogen bond plays a key role in increasing activity. In the meantime, the following interactions were formed (1): one pi-Alkyl interaction between the phenyl ring at 2-position of pyrimidine and residue ILE848; (2): two Alkyl interactions between the morpholine ring and residue TRP830 and VAL851, respectively; (3): one carbon hydrogen interaction between carbon atom at the morpholine ring and residue VAL851. The 3D model of the interaction between compound **14** and protein crystal structure of PI3Kα as shown in Fig. 8 **(B)** indicated that the active pockets of PI3Kα were occupied by compound **14**. These results could provide a molecular level foundation to illustrate that compound **14** could bind well at the active site of PI3Kα kinase and it is a potential inhibitor of PI3Kα.

Table 3
Percent of cell death induced by compound 14 (5.0 μM) on HCT-116 cells.

Compound No.	Apoptosis (%)			Necrosis (%)
	Total	Early	Late	
14	16.8	3.5	6.6	6.7
Cont. HCT-116	2.5	0.6	1.1	0.8

Furthermore, some physicochemical properties of the target compounds and GDC-0941 were predicted using free online website (http://www.molinspiration.com) for their adaptability with Lipinski's rule of five. As shown in Table 4, compounds **5** and **14** conformed well to the Lipinski's rule of five [29]. Both of them were predicted to possess strong drug resistance.

3. Conclusions

In the present study, four series of novel potent anticancer agents were designed and synthesized. The results of antiproliferative activities indicated that compound **14** significantly exhibits inhibitory activity against HT-29, MDA-MB-231, U87MG, PC-3 and HCT-116 cell lines with IC_{50} values of 1.78 μM, 1.02 μM, 1.98 μM, 0.41 μM and 0.22 μM, respectively. The SAR of these compounds indicated that thieno[3,2-*d*]pyrimidine and semicarbazone are optimal fragments. In addition, compound with hydroxyl at the 4-position on the terminal phenyl ring were more active. Moreover, the enzymatic assays suggested that the PI3Kα kinase might be the potential biological target for synthesized compounds. The cell apoptosis study found **14** is very effective in the induction of apoptosis in a dose-dependent manner. Cell cycle analysis of **14** by flow cytometry showed cell cycle arrest in G2/M phase. Docking simulation result showed that compound **14** could bind well at the PI3Kα active site. Further studies on the structural optimization of this series derivatives are currently underway in our laboratory.

4. Experimental

4.1. Chemistry

Unless otherwise specified, all materials were obtained from commercial suppliers and were used without further purification. Reactions' time and purity of the products were monitored by TLC on FLUKA silica gel aluminum cards (0.2 mm thickness) with fluorescent indicator 254 nm. Column chromatography was run on silica gel (200–300 mesh)

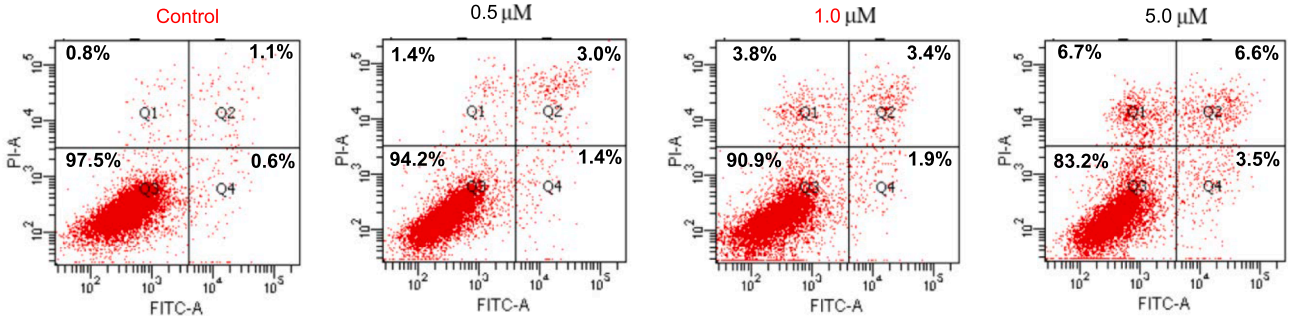

Fig. 5. Compound **14** induced apoptosis in HCT-116 cells. Cells were treated with various concentrations of **14** for 48 h and then analyzed the Annexin V-FITC/PI staining test by flow cytometry analysis. Values represent the mean ± S.D, n = 3. P < 0.05 versus the control. The percentage of cells in each part is indicated.

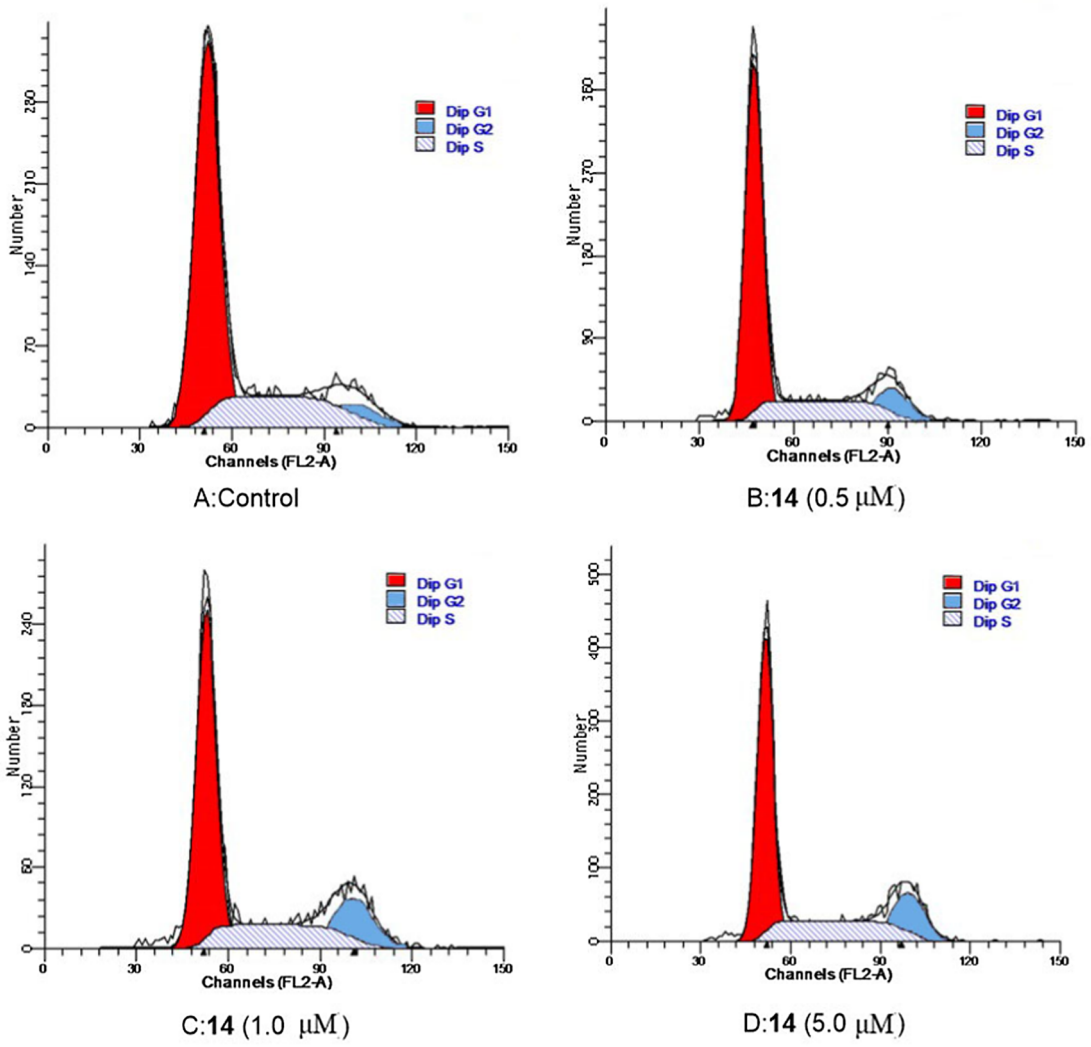

Fig. 6. Effect of compound **14** on the cell cycle distribution of HCT-116 cells. The experiments were performed three times and a representative experiment is shown.

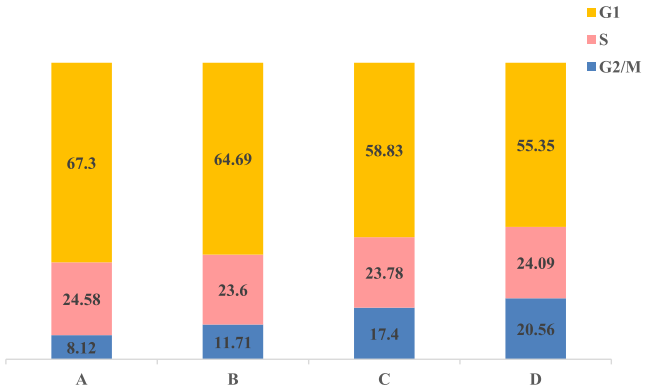

Fig. 7. Quantitative analysis of cell cycle distributions; (A) Non-treated cells as control group; (B) treated with **14** at 0.5 μM; (C) treated with **14** at 1.0 μM; (D) treated with **14** at 5.0 μM.

from Qingdao Ocean Chemicals (Qingdao, Shandong, China). All melting points were obtained on a Büchi Melting Point B-540 apparatus (Büchi Labortechnik, Flawil, Switzerland) and were uncorrected. Mass spectra (MS) were taken in ESI mode on Agilent 1100 LC–MS (Agilent, Palo Alto, CA, USA). ^{1}H NMR and ^{13}C NMR spectra were recorded on Bruker ARX-400, 400 MHz spectrometers (Bruker Bioscience, Billerica, MA, USA) with TMS as an internal standard.

*4.1.1. Preparation of 4-(4-morpholinothieno[3,2-d]pyrimidin-2-yl) benzaldehyde (**A$_1$**)*

*4.1.1.1. Preparation of thieno[3,2-d]pyrimidine-2,4-diol (**a**).* 20.0 g (0.13 mol) of methyl 3-amino-thiophene-2-carboxylate and 47.0 g (0.78 mol) of urea were intimately admixed with each other, and the resulted mixture was heated for two hours at 200 °C. A clear, brown molten mass was formed which solidified upon standing; the solid product was dissolved in warm 1 N sodium hydroxide, and the resulting solution was decolorized with charcoal and then acidified with 2 N hydrochloric acid. The crystalline precipitate formed thereby was collected by vacuum filtration, dried under reduced pressure to afford product **a** as a light yellow solid (18.5 g, 86.4%). MS (ESI) *m/z* (%): 191.0 $[M+Na]^+$.

*4.1.1.2. 2,4-Dichlorothieno[3,2-d]pyrimidine (**b**).* A mixture consisting of 16.0 g (0.095 mol) of thieno[3,2-*d*]pyrimidine-2,4-diol and 100 mL of phosphorus oxychloride was refluxed for 8 h whereby a clear solution was formed. Thereafter, the excess unreacted phosphorus oxychloride was evaporated in vacuo and the residual oil was poured into ice water. The precipitate formed under vigorous stirring conditions, thereby was collected by vacuum filtration, dried under reduced pressure to afford product **b** as a light yellow solid (15.8 g, 84.7%). MS (ESI) *m/z* (%): 205.1 $[M+H]^+$.

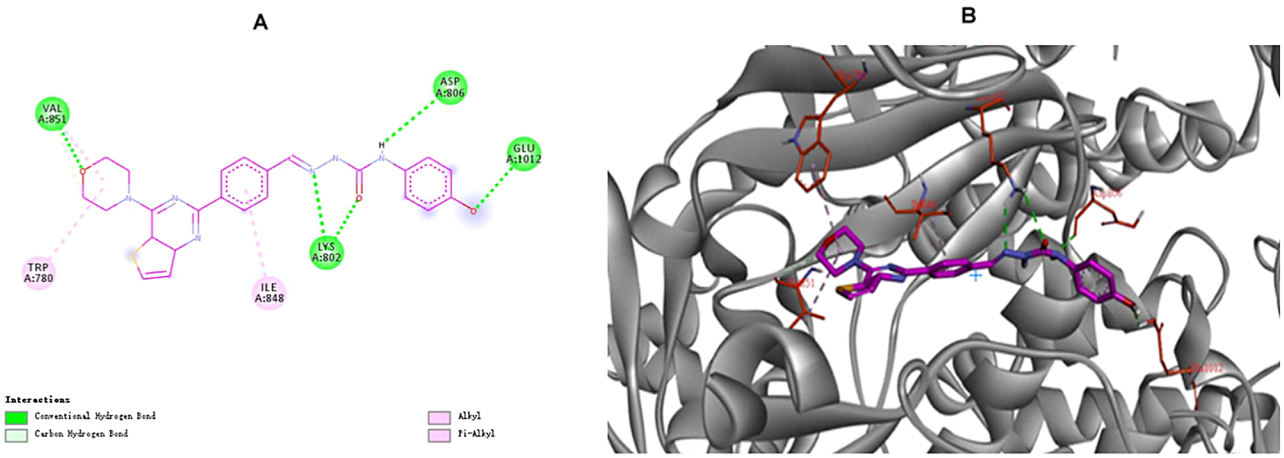

Fig. 8. Docking mode of compound **14** with protein crystal structure of PI3K. (A) 2D molecular docking model of compound **14** with protein crystal structure of PI3K. (B) 3D interaction map between compound **14** and binding sites of PI3Kα protein.

*4.1.1.3. 2,4-Dichlorothieno[3,2-d]pyrimidine (**c**).* 15.0 g (0.074 mol) of 2,4-dichlorothieno[3,2-*d*]pyrimidine were suspended in 150 mL of methyl alcohol at room temperature, then 16.8 mL (0.19 mol) of morpholine were added dropwise to the solution. Thereafter, the reaction mixture was stirred for 2 h at room temperature and then it was admixed with water. The precipitate formed and filtered, washed with water and dried under reduced pressure to afford product **c** as a light yellow solid (15.6 g, 82.7%); MS (ESI) *m/z* (%): 256.0 $[M+H]^+$.

*4.1.1.4. 4-(4-Morpholinothieno[3,2-d]pyrimidin-2-yl)benzaldehyde (**A_1**).* Palladium dichloro-bis(triphenylphosphine) 1.60 g (2.3 mmol) was added to a stirred solution of 9.80 g (0.065 mol) 4-formylbenzene boronic acid, 15.0 g (0.059 mol) 2,4-dichlorothieno[3,2-*d*]pyrimidine in 150 mL dioxane under a nitrogen atmosphere. The solution was purged with nitrogen and saturated cesium carbonate (0.15 mol) was added. The reaction mixture was stirred at 80 °C for 5 h, cooled to rt, and the precipitate was filtered and purified by silica gel column chromatography (eluent, CH_2Cl_2/MeOH = 30:1) to afford $\mathbf{A_1}$ as a pale solid. (14.8 g, 77.2%); MS (ESI) *m/z* (%): 326.2 $[M+H]^+$.

*4.1.2. Preparation of 4-(4-morpholinothieno[3,2-d]pyrimidin-2-yl) benzaldehyde (**A_2**)*

The preparation of the key intermediate $\mathbf{A_2}$ is the same as way to preparation A_1, So the synthesis method would not be listed here.

*4.1.2.1. Quinazoline-2,4-diol (**1**).* Yellow solid; Yield: 85.0%; MS (ESI) *m/z* (%): 163.1 $[M+H]^+$.

*4.1.2.2. 2,4-Dichloroquinazoline (**2**).* Light yellow solid; Yield: 77.9%; MS (ESI) *m/z* (%): 199.0 $[M+H]^+$.

*4.1.2.3. 4-(2-Chloroquinazolin-4-yl)morpholine (**3**).* Light yellow solid; Yield: 87.3%; MS (ESI) *m/z* (%): 250.2 $[M+H]^+$.

*4.1.2.4. 4-(4-Morpholinoquinazolin-2-yl)benzaldehyde (**A_2**).* Pale solid; Yield: 82.7%; MS (ESI) *m/z* (%): 320.2 $[M+H]^+$.

*4.1.3. General procedure for preparation of acylhydrazine intermediates (**B_1-B_3**)*

To a solution of an appropriate methyl esters (30 mmol) in 100 mL of toluene was added 80% hydrazine hydrate (0.30 mol) and the mixture was stirred at 80 °C for 2 h. After completion of reaction, it was allowed to cool, the precipitate was filtered and dried under reduced pressure to afford intermediates $\mathbf{B_1}$-$\mathbf{B_3}$

*4.1.3.1. 4-fluorobenzohydrazide (**B_1**).* White solid; Yield: 85.7%; MS (ESI) *m/z* (%): 155.2 $[M+H]^+$.

*4.1.3.2. 4-hydroxybenzohydrazide (**B_2**).* Light yellow solid; Yield: 82.4%; MS (ESI) *m/z* (%): 153.1 $[M+H]^+$.

*4.1.3.3. 4-methoxybenzohydrazide (**B_3**).* Light yellow solid; Yield: 79.5%; MS (ESI) *m/z* (%): 167.1 $[M+H]^+$.

*4.1.4. General procedure for preparation of hydrazinecarboxamide intermediates (**C_1-C_{13}**)*

A mixture of different substituted aniline (0.030 mol) and pyridine (0.060 mol) in CH_2Cl_2 (50 mL) was stirred at −10 °C for 5 min. Then phenyl carbonochloridate (0.090 mol) was added drop-wise to the solution and stirred for 5 h at 0 °C. When TLC showed the completion of the reaction, the mixture was concentrated under reduced pressure and the residue was dissolved in a solution of toluene (30.0 mL), and 80%

Table 4
Prediction of physicochemical properties[a] of the target compounds.

Compd	miLogP	TPSA	natoms	MW	nON	nOHNH	nviolations	nrotb	volume
Standard	< 5	< 140		< 500	< 5	< 5		≤10	
5	**4.17**	**99.95**	**33**	**459.33**	**8**	**2**	**0**	**5**	**394.05**
9	5.12	91.75	34	476.54	8	2	1	5	403.37
14	**4.48**	**111.97**	**34**	**474.55**	**9**	**3**	**0**	**5**	**406.45**
19	5.24	110.21	38	512.57	10	2	2	7	458.81
26	5.23	100.98	36	482.54	9	2	1	6	433.27
GDC-0941[b]	2.44	107.56	35	513.65	10	1	1	5	431.52

[a] miLogP: molinspiration predicted Log P; TPSA: topological polar surface area; natoms: no. of atoms; MW: molecular weight; nON: no. of hydrogen bond acceptors; nOHNH: no. of hydrogen bond donors; nviolations: no. of violations; nrotb: no. of rotatable bonds; volume: molar volume.
[b] Used as positive control.

hydrazine hydrate (0.30 mol). The mixture was heated to 80 °C for 2 h. After being cooled to rt, the precipitate was filtered and dried under reduced pressure to afford *intermediates* **C_1-C_{13}**.

*4.1.4.1. N-(3,4-dichlorophenyl)hydrazinecarboxamide (**C_1**).* White solid; Yield: 80.2%; MS (ESI) *m/z* (%): 220.3 $[M+H]^+$.

*4.1.4.2. N-(4-isopropylphenyl)hydrazinecarboxamide (**C_2**).* Light yellow solid; Yield: 84.4%; MS (ESI) *m/z* (%): 194.2 $[M+H]^+$.

*4.1.4.3. N-(4-fluorophenyl)hydrazinecarboxamide (**C_3**).* White solid; Yield: 89.5%; MS (ESI) *m/z* (%): 170.1 $[M+H]^+$.

*4.1.4.4. N-(2,4-dimethoxyphenyl)hydrazinecarboxamide (**C_4**).* Brown solid; Yield: 80.4%; MS (ESI) *m/z* (%): 212.1 $[M+H]^+$.

*4.1.4.5. N-(3-fluorophenyl)hydrazinecarboxamide (**C_5**).* White solid; Yield: 83.5%; MS (ESI) *m/z* (%): 170.1 $[M+H]^+$.

*4.1.4.6. N-phenylhydrazinecarboxamide (**C_6**).* White solid; Yield: 88.5%; MS (ESI) *m/z* (%): 152.1 $[M+H]^+$.

*4.1.4.7. N-(o-tolyl)hydrazinecarboxamide (**C_7**).* White solid; Yield: 82.7%; MS (ESI) *m/z* (%): 166.1 $[M+H]^+$.

*4.1.4.8. N -(4-hydroxyphenyl)hydrazinecarboxamide (**C_8**).* White solid; Yield: 73.4%; MS (ESI) *m/z* (%): 168.1 $[M+H]^+$.

*4.1.4.9. N-(2-chlorophenyl)hydrazinecarboxamide (**C_9**).* White solid; Yield: 82.5%; MS (ESI) *m/z* (%): 186.5 $[M+H]^+$.

*4.1.4.10. N-(4-bromophenyl)hydrazinecarboxamide (**C_{10}**).* White solid; Yield: 80.0%; MS (ESI) *m/z* (%): 230.1 $[M+H]^+$.

*4.1.4.11. N -(2-(trifluoromethyl)phenyl)hydrazinecarboxamide (**C_{11}**).* Light yellow solid; Yield: 72.9%; MS (ESI) *m/z* (%): 220.1 $[M+H]^+$.

*4.1.4.12. N-(3-(trifluoromethyl)phenyl)hydrazinecarboxamide (**C_{12}**).* White solid; Yield: 71.5%; MS (ESI) *m/z* (%): 220.1 $[M+H]^+$.

*4.1.4.13. N-(3-methoxyphenyl)hydrazinecarboxamide (**C_{13}**).* Brown solid; Yield: 90.5%; MS (ESI) *m/z* (%): 182.1 $[M+H]^+$.

*4.1.5. General procedure for preparation of target compounds (**4–26**)*

A mixture of **A1** or **A2** (0.63 mmol) and different substituted **B_1-B_3** or **C_1-C_{13}** (0.63 mmol) in EtOH (15 mL) was stirred at reflux for 2 h. After being cooled to rt, the precipitate was filtered and washed with EtOH (5 mL) and dried under reduced pressure to afford compounds **4–26** respectively.

*4.1.5.1. (E)-4-fluoro-N'-(4-(4-morpholinothieno[3,2-d]pyrimidin-2-yl) benzylidene)benzohydrazide (**4**).* White solid; Yield: 79.1%; M.p.: 278–279 °C; MS (ESI) *m/z*(%): 460.1 $[M-H]^-$; ^{1}H NMR (400 MHz, DMSO-d_6) δ (ppm): 11.81 (s, 1H), 8.49 (s, 2H), 8.48 (s, 1H), 8.27 (d, J = 5.4 Hz, 1H), 7.92 (d, J = 8.5 Hz, 2H), 7.83 (d, J = 7.4 Hz, 2H), 7.57 (d, J = 8.3 Hz, 2H), 7.54 (d, J = 5.5 Hz, 1H), 4.07 – 4.01 (m, 4H), 3.85 – 3.75 (m, 4H).

*4.1.5.2. (E)-4-hydroxy-N'-(4-(4-morpholinothieno[3,2-d]pyrimidin-2-yl) benzylidene)benzohydrazide (**5**).* Light yellow solid; Yield: 86.2%; M.p.: 265–268 °C; MS (ESI) *m/z*(%): 459.9 $[M+H]^+$; ^{1}H NMR (400 MHz, DMSO-d_6) δ (ppm): 11.71 (s, 1H), 10.15 (s, 1H), 8.47 (s, 3H), 8.26 (s, 1H), 7.81 (d, J = 6.5 Hz, 4H), 7.54 (s, 1H), 6.86 (d, J = 7.5 Hz, 2H), 4.01 (s, 4H), 3.80 (s, 4H).

*4.1.5.3. (E)-4-methoxy-N'-(4-(4-morpholinothieno[3,2-d]pyrimidin-2-yl) benzylidene)benzohydrazide (**6**).* Light yellow solid; Yield: 87.5%; M.p.: 286–288 °C; MS (ESI) *m/z*(%): 474.0 $[M+H]^+$; ^{1}H NMR (400 MHz, DMSO-d_6) δ (ppm): 11.81 (s, 1H), 8.49 (d, J = 8.6 Hz, 3H), 8.27 (d, J = 5.4 Hz, 1H), 7.92 (d, J = 8.5 Hz, 2H), 7.83 (d, J = 7.4 Hz, 2H), 7.55 (d, J = 5.3 Hz, 1H), 7.07 (d, J = 8.5 Hz, 2H), 4.02 (s, 4H), 3.83 (s, 3H), 3.81 (s, 4H).

*4.1.5.4. (E)-N-(3,4-dichlorophenyl)-2-(4-(4-morpholinothieno[3,2-d] pyrimidin-2-yl)benzylidene)hydrazine-1-carboxamide (**7**).* Yellow solid; Yield: 70.0%; M.p.: 275–277 °C; MS (ESI) *m/z* (%): 527.1 $[M+H]^+$. ^{1}H NMR (400 MHz, DMSO-d_6) δ 11.04 (s, 1H), 9.24 (s, 1H), 8.44 (d, J = 8.4 Hz, 2H), 8.25 (d, J = 5.5 Hz, 1H), 8.06 (d, J = 2.4 Hz, 1H), 8.01 (s, 1H), 7.95 (d, J = 8.4 Hz, 2H), 7.73 (dd, J = 8.9, 2.4 Hz, 1H), 7.55 (d, J = 3.3 Hz, 1H), 7.53 (s, 1H), 4.07 – 3.93 (m, 4H), 3.87 – 3.73 (m, 4H).

*4.1.5.5. (E)-N-(4-isopropylphenyl)-2-(4-(4-morpholinothieno[3,2-d] pyrimidin-2-yl)benzylidene)hydrazine-1-carboxamide (**8**).* Yellow solid; Yield: 80.1%; M.p.: 253–255 °C; MS (ESI) *m/z*(%): 501.1 $[M+H]^+$; ^{1}H NMR (400 MHz, DMSO-d_6) δ (ppm): 10.81 (s, 1H), 8.87 (s, 1H), 8.46 (d, J = 8.3 Hz, 2H), 8.27 (d, J = 5.5 Hz, 1H), 8.01 (s, 1H), 7.95 (d, J = 8.3 Hz, 2H), 7.58 (t, J = 7.0 Hz, 3H), 7.17 (d, J = 8.4 Hz, 2H), 4.02 (d, J = 4.4 Hz, 4H), 3.82 (d, J = 4.3 Hz, 4H), 2.85 (dt, J = 13.8, 6.9 Hz, 1H), 1.20 (d, J = 6.9 Hz, 6H).

*4.1.5.6. (E)-N-(4-fluorophenyl)-2-(4-(4-morpholinothieno[3,2-d] pyrimidin-2-yl)benzylidene) hydrazine-1-carboxamide (**9**).* Yellow solid; Yield: 73.0%; M.p.: 256–257 °C; MS (ESI) *m/z*(%): 477.0 $[M+H]^+$; ^{1}H NMR (400 MHz, DMSO-d_6) δ 10.86 (s, 1H), 9.01 (s, 1H), 8.44 (d, J = 8.4 Hz, 2H), 8.26 (d, J = 5.5 Hz, 1H), 8.00 (s, 1H), 7.94 (d, J = 8.4 Hz, 1H), 7.67 (dd, J = 9.1, 5.0 Hz, 2H), 7.54 (d, J = 5.5 Hz, 1H), 7.13 (t, J = 8.9 Hz, 2H), 4.05 – 3.96 (m, 4H), 3.84 – 3.75 (m, 4H).

*4.1.5.7. (E)-N-(2,4-dimethoxyphenyl)-2-(4-(4-morpholinothieno[3,2-d] pyrimidin-2-yl)benzylidene)hydrazine-1-carboxamide (**10**).* Yellow solid; Yield: 74.9%; M.p.: 278–259 °C; MS (ESI) *m/z* (%): 519.2 $[M+H]^+$. ^{1}H NMR (400 MHz, DMSO-d_6) δ 10.92 (s, 1H), 8.54 (s, 1H), 8.47 (d, J = 8.4 Hz, 2H), 8.25 (d, J = 5.5 Hz, 1H), 8.00 (s, 1H), 7.90 (d, J = 8.8 Hz, 1H), 7.77 (d, J = 8.4 Hz, 2H), 7.52 (d, J = 5.5 Hz, 1H), 6.65 (d, J = 2.6 Hz, 1H), 6.49 (dd, J = 8.8, 2.6 Hz, 1H), 4.05 – 3.96 (m, 4H), 3.91 (s, 3H), 3.84 – 3.76 (m, 4H), 3.73 (s, 3H).

*4.1.5.8. (E)-N-(3-fluorophenyl)-2-(4-(4-morpholinothieno[3,2-d] pyrimidin-2-yl)benzylidene)hydrazine-1-carboxamide (**11**).* White solid; Yield: 81.4%; M.p.: 255–256 °C; MS (ESI) *m/z*(%): 477.0 $[M+H]^+$; ^{1}H NMR (400 MHz, DMSO-d_6) δ (ppm): 10.95 (s, 1H), 9.13 (s, 1H), 8.45 (d, J = 8.3 Hz, 2H), 8.25 (d, J = 5.5 Hz, 1H), 8.01 (s, 1H), 7.95 (d, J = 8.4 Hz, 2H), 7.64 (d, J = 12 Hz, 1H), 7.54 (d, J = 5.5 Hz, 1H), 7.51 (d, J = 8.5 Hz, 1H), 7.32 (dd, J = 15.3, 8.0 Hz, 1H), 6.82 (td, J = 8.4, 2.1 Hz, 1H), 4.09 – 3.87 (m, 4H), 3.87 – 3.68 (m, 4H).

*4.1.5.9. (E)-2-(4-(4-morpholinothieno[3,2-d]pyrimidin-2-yl)benzylidene)-N-phenylhydrazine-1-carboxamide (**12**).* Light yellow solid; Yield: 81.3%; M.p.: 251–253 °C; MS (ESI) *m/z*(%): 459.0 $[M+H]^+$; ^{1}H NMR (400 MHz, DMSO-d_6) δ (ppm): 10.84 (s, 1H), 8.94 (s, 1H), 8.44 (d, J = 8.4 Hz, 2H), 8.26 (d, J = 5.5 Hz, 1H), 8.00 (s, 1H), 7.94 (d, J = 8.4 Hz, 2H), 7.66 (d, J = 7.7 Hz, 2H), 7.54 (d, J = 5.5 Hz, 1H), 7.29 (t, J = 7.9 Hz, 2H), 7.01 (t, J = 7.3 Hz, 1H), 4.06 – 3.94 (m, 4H), 3.88 – 3.73 (m, 4H).

*4.1.5.10. (E)-2-(4-(4-morpholinothieno[3,2-d]pyrimidin-2-yl) benzylidene)-N-(o-tolyl)hydrazine-1-carboxamide (**13**).* Light yellow solid; Yield: 81.0%; M.p.: 245–247 °C; MS (ESI) *m/z*(%): 470.8 $[M-H]^-$; ^{1}H NMR (400 MHz, DMSO-d_6) δ (ppm): 10.90 (s, 1H), 8.55 (s, 1H), 8.44 (d, J = 8.1 Hz, 2H), 8.25 (d, J = 5.5 Hz, 1H), 8.00 (s, 1H), 7.86 (d, J = 8.2 Hz, 2H), 7.69 (d, J = 7.8 Hz, 1H), 7.52 (d, J = 5.4 Hz,

1H), 7.26 – 7.13 (m, 2H), 7.03 (t, J = 7.4 Hz, 1H), 4.00 (s, 4H), 3.79 (s, 4H), 2.29 (s, 3H).

4.1.5.11. (E)-N-(4-hydroxyphenyl)-2-(4-(4-morpholinothieno[3,2-d] pyrimidin-2-yl)benzylidene)hydrazine-1-carboxamide ***(14)***. Yellow solid; Yield: 71.3%; M.p.: 266–267 °C; MS (ESI) m/z (%): 475.2 $[M+H]^+$. ^{1}H NMR (600 MHz, DMSO-d_6) δ (ppm) 10.71 (s, 1H), 9.13 (s, 1H), 8.72 (s, 1H), 8.45 (d, J = 8.5 Hz, 2H), 8.27 (d, J = 5.5 Hz, 1H), 7.99 (s, 1H), 7.94 (d, J = 8.5 Hz, 2H), 7.55 (d, J = 5.5 Hz, 1H), 7.40 (d, J = 8.8 Hz, 2H), 6.72 (d, J = 8.8 Hz, 2H), 4.02 (t, J = 4.9 Hz, 4H), 3.82 (t, J = 4.8 Hz, 4H). ^{13}C NMR (150 MHz, DMSO-d_6) δ (ppm)162.79, 159.01, 158.19, 153.64, 153.47, 140.12, 138.95, 136.46, 134.36, 130.76, 128.24, 127.26, 125.22, 122.68, 115.24, 112.70, 66.36, 46.27.

4.1.5.12. (E)-N-(2-chlorophenyl)-2-(4-(4-morpholinothieno[3,2-d] pyrimidin-2-yl)benzylidene)hydrazine-1-carboxamide ***(15)***. White solid; Yield: 73.5%; M.p.: 252–253 °C; MS (ESI) m/z(%): 491.1 $[M-H]^-$; ^{1}H NMR (600 MHz, DMSO-d_6) δ (ppm) 10.90 (s, 1H), 8.56 (s, 1H), 8.46 (d, J = 8.5 Hz, 2H), 8.27 (d, J = 5.5 Hz, 1H), 8.03 (s, 1H), 7.88 (d, J = 8.4 Hz, 2H), 7.71 (dd, J = 8.0, 1.3 Hz, 1H), 7.54 (d, J = 5.5 Hz, 1H), 7.24 (dd, J = 7.4, 1.5 Hz, 1H), 7.20 (s, 1H), 7.06 (dd, J = 7.4, 1.3 Hz, 1H), 4.03 (t, J = 4.9 Hz, 4H), 3.86 – 3.77 (m, 4H).

4.1.5.13. (E)-4-methoxy-N'-(4-(4-morpholinoquinazolin-2-yl)benzylidene) benzohydrazide ***(16)***. Yellow green solid; Yield: 81.0%; M.p.: 233–235 °C; MS (ESI) m/z(%): 468.4 $[M+H]^+$; ^{1}H NMR (400 MHz, DMSO-d_6) δ (ppm): 11.81 (s, 1H), 8.55 (d, J = 8.2 Hz, 2H), 8.51 (s, 1H), 8.05 (d, J = 8.3 Hz, 1H), 7.96 – 7.88 (m, 3H), 7.83 (t, J = 7.7 Hz, 3H), 7.53 (t, J = 7.5 Hz, 1H), 7.06 (d, J = 8.8 Hz, 2H), 3.83 (s, 11*H*).

4.1.5.14. (E)-4-fluoro-N'-(4-(4-morpholinoquinazolin-2-yl)benzylidene) benzohydrazide ***(17)***. Yellow solid; Yield:78.5%; M.p.: 201–203 °C; MS (ESI) m/z(%): 453.9 $[M-H]^-$; ^{1}H NMR (400 MHz, DMSO-d_6) δ (ppm): 11.95 (s, 1H), 8.56 (d, J = 8.1 Hz, 2H), 8.51 (s, 1H), 8.09 – 7.95 (m, 3H), 7.86 (dq, J = 15.3, 7.8 Hz, 4H), 7.53 (t, J = 7.3 Hz, 1H), 7.38 (t, J = 8.6 Hz, 2H), 3.83 (s, 8H).

4.1.5.15. (E)-N-(4-isopropylphenyl)-2-(4-(4-morpholinoquinazolin-2-yl) benzylidene)hydrazine-1-carboxamide ***(18)***. Yellow solid; Yield: 84.2%; M.p.: 247–249 °C; MS (ESI) m/z(%): 495.3 $[M+H]^+$; ^{1}H NMR (400 MHz, DMSO-d_6) δ (ppm):10.84 (s, 1H), 8.88 (s, 1H), 8.53 (d, J = 8.3 Hz, 2H), 8.06 (d, J = 8.3 Hz, 1H), 8.02 (s, 1H), 7.99 (d, J = 8.3 Hz, 2H), 7.92 (d, J = 8.3 Hz, 1H), 7.85 (t, J = 7.6 Hz,1H), 7.58 (d, J = 8.5 Hz, 2H), 7.54 (t, J = 7.6 Hz, 1H), 7.18 (d, J = 8.5 Hz, 2H), 3.85 (s, 8H), 2.90 – 2.80 (m, 1H), 1.20 (d, J = 6.9 Hz, 6H).

4.1.5.16. (E)-N-(2,4-dimethoxyphenyl)-2-(4-(4-morpholinoquinazolin-2-yl)benzylidene)hydrazine-1-carboxamide ***(19)***. Yellow solid; Yield: 83.7%; M.p.: 247–249 °C; MS (ESI) m/z(%): 513.2 $[M+H]^+$; ^{1}H NMR (400 MHz, DMSO-d_6) δ (ppm): 10.94 (s, 1H), 8.55 (s, 1H), 8.53 (s, 2H), 8.04 (d, J = 8.3 Hz, 1H), 8.01 (s, 1H), 7.90 (d, J = 9.0 Hz, 2H), 7.84 (d, J = 7.6 Hz, 1H), 7.80 (d, J = 8.1 Hz, 2H), 7.52 (t, J = 7.5 Hz, 1H), 6.66 (d, J = 1.8 Hz, 1H), 6.50 (dd, J = 8.7, 1.9 Hz, 1H), 3.92 (s, 3H), 3.83 (s, 8H), 3.74 (s, 3H).

4.1.5.17. (E)-N-(3-fluorophenyl)-2-(4-(4-morpholinoquinazolin-2-yl) benzylidene)hydrazine-1-carboxamide ***(20)***. Yellow green solid; Yield: 80.2%; M.p.: 259–260 °C; MS (ESI) m/z(%): 469.0 $[M-H]^-$; ^{1}H NMR (400 MHz, DMSO-d_6) δ (ppm): 10.98 (s, 1H), 9.14 (s, 1H), 8.52 (d, J = 8.3 Hz, 2H), 8.04 (d, J = 8.9 Hz, 2H), 7.98 (d, J = 8.3 Hz, 2H), 7.90 (d, J = 8.2 Hz, 1H), 7.82 (t, J = 7.6 Hz, 1H), 7.66 (d, J = 12.0 Hz, 1H), 7.57 – 7.46 (m, 2H), 7.32 (dd, J = 15.4, 8.0 Hz, 1H), 6.83 (dd, J = 11.8, 5.0 Hz, 1H), 3.83 (s, 8H).

4.1.5.18. (E)-N-(4-bromophenyl)-2-(4-(4-morpholinoquinazolin-2-yl) benzylidene)hydrazine-1-carboxamide ***(21)***. Yellow green solid; Yield: 81.3%; M.p.: 264–266 °C; MS (ESI) m/z(%): 531.4 $[M+H]^+$; ^{1}H NMR (400 MHz, DMSO-d_6) δ (ppm): 10.95 (s, 1H), 9.09 (s, 1H), 8.51 (d, J = 8.2 Hz, 2H), 8.04 (d, J = 8.5 Hz, 1H), 8.01 (s, 1H), 7.97 (d, J = 8.2 Hz, 2H), 7.90 (d, J = 8.3 Hz, 1H), 7.82 (t, J = 7.6 Hz, 1H), 7.69 (d, J = 8.7 Hz, 2H), 7.52 (t, J = 7.7 Hz, 1H), 7.47 (d, J = 8.7 Hz, 2H), 3.83 (s, 8H).

4.1.5.19. (E)-2-(4-(4-morpholinoquinazolin-2-yl)benzylidene)-N-(o-tolyl) hydrazine-1-carboxamide ***(22)***. White solid; Yield: 80.6%; M.p.: 237–240 °C; MS (ESI) m/z(%): 467.2 $[M+H]^+$; ^{1}H NMR (400 MHz, DMSO-d_6) δ (ppm): 10.92 (s, 1H), 8.57 (s, 1H), 8.51 (d, J = 8.2 Hz, 2H), 8.05 (s, 1H), 8.05 (s, 1H), 8.02 (s, 1H), 7.90 (d, J = 8.4 Hz, 2H), 7.82 (t, J = 7.5 Hz, 1H), 7.69 (d, J = 7.9 Hz, 1H), 7.52 (t, J = 7.5 Hz, 1H), 7.23 (d, J = 7.4 Hz, 1H), 7.18 (t, J = 7.6 Hz, 1H), 7.03 (t, J = 7.4 Hz, 1H), 3.82 (s, 8H), 2.30 (s, 3H).

4.1.5.20. (E)-2-(4-(4-morpholinoquinazolin-2-yl)benzylidene)-N-phenylhydrazine-1-carboxamide ***(23)***. White solid; Yield: 82.3%; M.p.: 247–249 °C; MS (ESI) m/z(%): 453.2 $[M+H]^+$; ^{1}H NMR (400 MHz, DMSO-d_6) δ (ppm): 10.87 (s, 1H), 8.95 (s, 1H), 8.51 (d, J = 8.4 Hz, 2H), 8.04 (d, J = 8.3 Hz, 1H), 8.01 (s, 1H), 7.97 (d, J = 8.4 Hz, 2H), 7.90 (d, J = 7.9 Hz, 1H), 7.82 (t, J = 7.6 Hz, 1H), 7.67 (d, J = 7.8 Hz, 2H), 7.52 (t, J = 7.5 Hz, 1H), 7.30 (t, J = 7.9 Hz, 2H), 7.01 (t, J = 7.3 Hz, 1H), 3.83 (s, 8H).

4.1.5.21. (E)-2-(4-(4-morpholinoquinazolin-2-yl)benzylidene)-N-(2-(trifluoromethyl)phenyl)hydrazine-1-carboxamide ***(24)***. White solid; Yield: 78.2%; Mp: 230–231 °C; MS (ESI) m/z (%): 521.3 $[M+H]^+$. ^{1}H NMR (400 MHz, DMSO-d_6) δ (ppm) 11.28 (s, 1H), 8.87 (d, J = 30.0 Hz, 1H), 8.56 (d, J = 29.0 Hz, 2H), 8.19 (s, 1H), 8.06 (s, 2H), 7.86 (d, J = 23.0 Hz, 4H), 7.70 (d, J = 17.5 Hz, 2H), 7.53 (s, 1H), 7.30 (s, 1H), 3.84 (s, 8H).

4.1.5.22. (E)-2-(4-(4-morpholinoquinazolin-2-yl)benzylidene)-N-(3-(trifluoromethyl)phenyl)hydrazine-1-carboxamide ***(25)***. Yellow solid; Yield: 70.0%; Mp: 232–233 °C; MS (ESI) m/z (%): 521.3 $[M+H]^+$. ^{1}H NMR (400 MHz, DMSO) δ (ppm) 11.03 (s, 1H), 9.29 (s, 1H), 8.53 (d, J = 8.4 Hz, 2H), 8.15 (s, 1H), 8.02 (dd, J = 19.7, 7.5 Hz, 5H), 7.90 (d, J = 7.8 Hz, 1H), 7.83 (t, J = 7.6 Hz, 1H), 7.57 – 7.48 (m, 2H), 7.35 (d, J = 7.7 Hz, 1H), 3.83 (s, 8H).

4.1.5.23. (E)-N-(3-methoxyphenyl)-2-(4-(4-morpholinoquinazolin-2-yl) benzylidene)hydrazine-1-carboxamide ***(26)***. Light yellow solid; Yield: 78.3%; M.p.: 228–230 °C; MS (ESI) m/z(%): 483.4 $[M+H]^+$; ^{1}H NMR (400 MHz, DMSO-d_6) δ (ppm): 10.87 (s, 1H), 8.91 (s, 1H), 8.52 (d, J = 8.4 Hz, 2H), 8.05 (d, J = 8.3 Hz, 1H), 8.01 (s, 1H), 7.97 (d, J = 8.4 Hz, 2H), 7.91 (d, J = 8.5 Hz, 1H), 7.83 (t, J = 7.6 Hz, 1H), 7.52 (t, J = 7.6 Hz, 1H), 7.35 (t, J = 2.0 Hz, 1H), 7.28 (d, J = 8.1 Hz, 1H), 7.19 (t, J = 8.1 Hz, 1H), 6.59 (dd, J = 8.0, 2.0 Hz, 1H), 3.83 (s, 8H), 3.74 (s, 3H).

4.2. Pharmacology

4.2.1. In vitro antiproliferative assays

The antiproliferative activities of compounds **4**–**26** and were evaluated against HT-29, MDA-MB-231, U87MG, PC-3 and HCT-116 cell lines by the standard MTT assay in vitro, with GDC-0941 as the positive controls. The cancer cell lines were cultured in minimum essential medium (MEM) supplement with 10% fetal bovine serum (FBS). Approximate 4×10^3 cells, suspended in MEM medium, were plated into each well of a 96-well plate and incubated in 5% CO_2 at 37 °C for 24 h. The tested compounds at the indicated final concentrations were added to the culture medium and incubated for 72 h. Fresh MTT was added to each well at the terminal concentration of 5 μg/mL, and incubated with cells at 37 °C for 4 h. The formazan crystals in each well were dissolved in 100 μL DMSO, and the absorbency at 492 nm (for

absorbance of MTT formazan) and 630 nm (for the reference wavelength) was measured with an ELISA reader. All of the compounds were tested three times in each of the cell lines. The results, expressed as IC_{50} (inhibitory concentration 50%), were the averages of three determinations and calculated relative to the vehicle (DMSO) control by the Bacus Laboratories Incorporated Slide Scanner (Bliss) software.

4.2.2. In vitro enzymatic assays [28]

The in vitro enzymatic assays of compound **14** were evaluated by homogeneous time-resolved fluorescence (HTRF) assay. Briefly, 20 μg/mL poly (Glu, Tyr) 4:1 (Sigma) was preloaded as a substrate in 384-well plates. Then 50 μL of 10 mM ATP (Invitrogen) solution diluted in kinase reaction buffer (50 mM HEPES, Ph 7.0, 1 mM DTT,1 mM $MgCl_2$, 1 mM $MnCl_2$, 0.1% NaN_3) was added to each well. Various concentrations of compounds were diluted in 10 μL of 1% DMSO (v/v), with blank DMSO solution as the negative control. The kinase reaction was initiated by the addition of purified tyrosine kinase proteins diluted in 39 μL of kinase reaction buffer solution. Reactions were incubated for 30 min at 25 °C and stopped by the addition of 5 μL Streptavidin-XL665 and 5 μL Tk Antibody Cryptate working solution to all of wells. The plate was read by Envision (PerkinElmer) at 320 nm and 615 nm. IC_{50} values were calculated from the inhibition curves.

4.2.3. Flow cytometry

The HCT-116 cells were seeded in 6-well plates at a seeding density of 105 cells per mL. Twelve hours later, various concentrations of compound **14** were added. Cells were treated with compound **14** for 48 h. Then cells were transferred to EP tubes and washed three times with PBS buffer. Then the procedures according to the operating instructions of the kit were followed. Ultimately, cell apoptosis was analyzed using Annexin-V and propidium iodide (PI) double staining by flow cytometry. Early apoptotic cells were defined as Annexin-V positive/PI negative, late apoptotic cells as Annexin-V/PI-double positive and necrotic cells as Annexin-V positive/PI positive.

4.2.4. Cell cycle distribution analysis

The effects of compounds on cell cycle progression were determined using a standard propidium iodide (PI) staining procedure followed by flow cytometry analysis. Briefly, HCT-116 cells were seeded in six-well plates (5×10^4/well) and then treated with different concentrations of **14** for 48 h. The cells were collected and washed twice with ice cold PBS, then fixed in ice-cold 70% (v/v) ethanol overnight at 4 °C. The cells were washed again by PBS, and then the cell DNA was stained with 400 μL PI (Beyotime) for 10 min. Data acquisition and analysis were performed using a flow cytometer.

4.2.5. Molecular docking study

The crystal structure of PI3K (PDB entry code: 4L23) in complex with PI-103 was used for molecular modeling. The molecular docking procedure was performed by using C-DOCKER protocol within Accelrys Discovery Studio Visualizer 4.0. For enzyme preparation, the hydrogen atoms were added. The whole PI3K enzyme was defined as a receptor and the site sphere was selected on the basis of the ligand binding location of PI-103. Compound PI-103 was removed and compound **14** was placed. Accelrys Discovery Studio Visualizer 4.0 was used for graphic display.

Acknowledgements

This work was supported by National Natural Science Foundation of China (No. 81573296) and Liaoning BaiQianWan Talents Program “Design, synthesis and biological evaluation of compounds containing diaryl urea moiety as PI3K /mTOR dual inhibitors”.

References

[1] K.R. Auger, L.A. Serunian, S.P. Soltoff, P. Libby, L.C. Cantley, Cell 57 (1989) 167–175.
[2] L.C. Cantley, Science 296 (2002) 1655–1657.
[3] M. Whitman, C.P. Downes, M. Keeler, T. Keller, L.C. Cantley, Nature 332 (1988) 644–646.
[4] T.F. Franke, D.L. Kaplan, L.C. Cantley, Cell 88 (1997) 435–437.
[5] P.R. Shepherd, D.J. Withers, K. Siddle, Biochem. J. 333 (1998) 471–490.
[6] M. Lindvall, C. Mcbride, M. Mckenna, T.G. Gesner, A. Yabannavar, K. Wong, S. Lin, A. Walter, C.M. Shafer, ACS Med. Chem. Lett. 2 (2011) 720–723.
[7] Y. Ni, A. Gopalsamy, D. Cole, Y. Hu, R.A. Denny, M. Ipek, J. Liu, J. Lee, J.P. Hall, M. Luong, J.L. Telliez, Bioorg. Med. Chem. Lett. 21 (2011) 5952–5956.
[8] T.P. Heffron, M. Berry, G. Castanedo, C. Chang, I. Chuckowree, J. Dotson, A. Folkes, J. Gunzner, J. Lesnick, C. Lewis, S. Mathieu, J. Nonomiya, A.G. Olivero, J. Pang, D. Peterson, L. Salphati, D. Sampath, S. Sideris, D.P. Sutherlin, V. Tsui, N.C. Wan, S. Wang, S. Wong, B. Zhu, Bioorg. Med. Chem. Lett. 20 (2010) 2408–2411.
[9] C. Yu, P. Chiang, P. Lu, M. Kuo, W. Wen, P. Chen, J. Guh, J. Med. Chem. 53 (2010) 1086–1097.
[10] B. Lannutti, S.A. Meadows, S.E. Herman, A. Kashishian, B.H. Steiner, A.J. Johnson, J.C. Byrd, J.W. Tyner, M. Loriaux, M. Deininger, B.J. Druker, K.D. Puri, R.G. Ulrich, N.A. Giese, Blood 117 (2011) 591–594.
[11] N.S. Shetty, R.S. Lamani, I.A. Khazi, J. Chem. Sci. 121 (2009) 301–307.
[12] A.B. Elgazzar, H.A. Hussein, H.N. Hafez, Acta Pharm. 57 (2007) 395–411.
[13] A. Folkes, K. Ahmadi, W.K. Alderton, S. Alix, S. Baker, G. Box, I. Chuckowree, P.A. Clarke, P. Depledge, S.A. Eccles, L.S. Friedman, A. Hayes, T.C. Hancox, A. Kugendradas, L. Lensun, P. Moore, A.G. Olivero, J. Pang, S. Patel, G. Perglwilson, F.L. Raynaud, A. Robson, N. Saghir, L. Salphati, S. Sohal, M. Ultsch, M. Valenti, H.J.A. Wallweber, N.C. Wan, C. Wiesmann, P. Workman, A. Zhyvoloup, M. Zvelebil, S.J. Shuttleworth, J. Med. Chem. 51 (2008) 5522–5532.
[14] T.T. Junttila, R.W. Akita, K. Parsons, C. Fields, G.L. Phillips, L.S. Friedman, D. Sampath, M.X. Sliwkowski, Cancer Cell 15 (2009) 429–440.
[15] A. Palazzo, S. Herter, L.S. Grosmaire, R. Jones, C.R. Frey, F. Limani, M. Bacac, P. Umana, R.J. Oldham, M.J. Marshall, K.L. Cox, A.H. Turaj, M.S. Cragg, C. Klein, M.J. Carter, S. Tannheimer, J. Immunol. 200 (2018) 2304–2312.
[16] M. Andrs, J. Korabecny, D. Jun, Z. Hodny, J. Bartek, K. Kuca, J. Med. Chem. 58 (2015) 41–47.
[17] Y. Fan, H. Ding, D. Liu, H. Song, Y. Xu, J. Wang, Bioorg. Med. Chem. 26 (2018) 1675–1685.
[18] C.A. Fraga, E.J. Barreiro, Curr. Med. Chem. 13 (2006) 167–198.
[19] R.T. Sudo, G. Zapatasudo, E.J. Barreiro, Br. J. Pharmacol. 134 (2001) 603–613.
[20] J.D. Silva, D. Gabrielcosta, R.T. Sudo, H. Wang, L. Groban, E.B. Ferraz, J. Nascimento, C.A.M. Fraga, E.J. Barreiro, G. Zapatasudo, Drug. Des. Devel. Ther. 11 (2017) 553–562.
[21] D.N. Amaral, B.C. Cavalcanti, D.P. Bezerra, P.M. Ferreira, R.D. Castro, J.R. Sabino, C.M. Machado, R. Chammas, C. Pessoa, C.M. Santanna, E.J. Barreiro, L.M. Lima, Plos One 9 (2014) e85380.
[22] D.A. Rodrigues, G.A. Ferreirasilva, A.C. Ferreira, R.A. Fernandes, J.K. Kwee, C.M. Anna, M. Ionta, C.A. Fraga, J. Med. Chem. 59 (2016) 655–670.
[23] A.E. Kummerle, M. Schmitt, S.V. Cardozo, C. Lugnier, P. Villa, A.B. Lopes, N.C. Romeiro, H. Justiniano, M.A. Martins, C.A. Fraga, J. Bourguignon, E.J. Barreiro, J. Med. Chem. 55 (2012) 7525–7545.
[24] P.W. Lucas, J.M. Schmit, Q.P. Peterson, D.C. West, D.C. Hsu, C.J. Novotny, L. Dirikolu, M.I. Churchwell, D.R. Doerge, L.D. Garrett, P.J. Hergenrother, T.M. Fan, Invest. New. Drug. 29 (2011) 901–911.
[25] B. Qi, H. Tao, D. Wu, J. Bai, Y. Shi, P. Gong, Archiv der Pharmazie. 346 (2013) 596–609.
[26] Woitun E., Ohnacker G., Narr B., Horch U., Kadatz R., US 3763156, 1973-12-02.
[27] Lambert W., Crouse G., Sparks T., Cudworth D., WO 2011017513, 2011-02-10.
[28] Z. Liu, Y. Wang, H. Lin, D. Zuo, L. Wang, Y. Zhao, P. Gong, Eur. J. Med. Chem. 85 (2014) 215–227.
[29] Z. Lv, W. He, X. Tian, J. Kang, Y. Liu, Y. Peng, L. Zheng, Q. Wang, W. Yu, J. Chang, Eur. J. Med. Chem. 101 (2015) 103–110.